Chinese Chemical Letters 34 (2023) 108044

Contents lists available at ScienceDirect

Chinese Chemical Letters

journal homepage: www.elsevier.com/locate/cclet

In situ synthesized homochiral dysprosium-oxo clusters with threonine Schiff bases

Song Peng[a,1], Xiaoming Ouyang[a,1], Yihan Wang[a,1], Qinghu Teng[a,*], Yan Li[a], Xiuqing Zhang[a], Zhaobo Hu[b], Kai Wang[a,*], Fupei Liang[a,*]

[a] *Guangxi Key Laboratory of Electrochemical and Magnetochemical Functional Materials, College of Chemistry and Bioengineering, Guilin University of Technology, Guilin 541004, China*

[b] *Jiangxi Provincial Key Laboratory of Functional Molecular Materials Chemistry, Jiangxi University of Science and Technology, Ganzhou 341000, China*

ARTICLE INFO

Article history:
Received 23 October 2022
Accepted 5 December 2022
Available online 7 December 2022

Keywords:
Chirality
Lanthanide-oxo cluster
In situ synthesis
Threonine Schiff bases
Hydrolysis
Magnetic properties

ABSTRACT

Chiral high-nuclearity lanthanide (4f) clusters have shown fantastic properties in various fields. However, their synthesis is still of great challenge. Herein, we report two pairs of enantiomers of high-nuclearity Dy-oxo clusters synthesized through *in situ* strategy. They are $[Dy_{18}(^{R/S}Hftp)_4\ (^{R/S}H_2btp)_4(\mu_2\text{-}OH)_8(\mu_3\text{-}OH)_{20}(\mu_6\text{-}O)(NO_3)_4(\mu\text{-}H_2O)_8]\cdot$[solvents] (**1R** and **1S**) and $[Dy_9(^{R/S}Hftp)_2\ (^{R/S}H_2btp)_2(OAc)_6(\mu_3\text{-}OH)_{10}(H_2O)_6](OAc)\cdot$[solvents] (**2R** and **2S**), where $^{R/S}Hftp^{2-}$ and $^{R/S}H_2btp^{3-}$ represent *in situ* formed 2-formyl-6-[*N*-(*threonine*)*iminomethyl*]-4-methylphenol and 2,6-bis[*N*-(*threonine*)*iminomethyl*]-4-methylphenol anions, respectively. These *in situ* formed clusters were endowed with not only homochirality *via* introducing $^{R/S}Hftp^{2-}$ and $^{R/S}H_2btp^{3-}$ ligands, but also rich oxo-bridges by controlling the hydrolysis of Dy^{III} ions. Different anions from Dy^{III} salts further induced structural variation between two sets of clusters. **1R** and **1S** feature an unprecedent four-blade propeller shaped $\{Dy_{18}\}$ core, whose centered octahedral $\{Dy_6\}$ unit are surrounded by four triangular $\{Dy_3\}$ units. Strikingly, they represent the second largest chiral 4f cluster species so far. **2R** and **2S** display a sandglass-like $\{Dy_9\}$ skeleton that consist of two square pyramid $\{Dy_5\}$ units sharing a Dy^{III} vertex. Magnetic investigation revealed possible antiferromagnetic interactions between the Dy^{III} centers in these clusters.

Polymetallic coordination clusters have attracted great interest over the past few years due to their applications in various fields [1–3]. One of the most intriguing species among their family is those featuring chirality. Apart from possessing general properties of achiral systems, chiral clusters can also display other interesting functions brought by chiral topologies, such as ferroelectricity [4,5], multiferroic [6], magnetic circular dichroism [7], circularly polarized luminescence (CPL) [8,9], chiral separation and catalysis [10,11]. Among them, chiral high-nuclearity 4f clusters are paid much more attentions probably due to their impressive topologies and fantastic properties resulted from the integration of functional homochiral ligands with the metal centers featuring 4f electron shell. For examples, the reported triple helix $\{La_8\}$ could fix CO_2 efficiently [12], circular $\{Eu_8\}$ helicates exhibit remarkable visible CPL activity with a high luminescence dissymmetry factor $|g_{lum}|$ of 1.25 [13], and $\{La_{12}\}$ shows an unprecedented homochiral octahedral "cage in cage" topology and remarkable enantioselective separation abilities [14]. In comparison with those based on 3d and 3d-4f metal centers, however, the reported chiral 4f clusters with the nuclearity higher than 10 are still limited at present (Table S2 in Supporting information) [14–18]. Thus, the exploration of novel chiral high-nuclearity 4f clusters is of great importance, whether from the view of their potential application or from the present scarcity.

As a kind of versatile molecules, Schiff base compounds have shown broad applications in different fields such as biology and medicine [19,20]. It is also noteworthy that they have demonstrated extraordinary capabilities in the construction of high-nuclearity metal clusters. In recent years, a series of novel Schiff base ligands have been designed and synthesized by our group and have been put into the exploration of high-nuclearity 4f clusters. *N*,*N*′-Bis(*o*-vanillidene)pyridine-2,6-dicarbohydrazide *N*-oxide is just one of them (H_4ovpho, Scheme 1, top). Its structural specificity

* Corresponding authors.
E-mail addresses: 2020130@glut.edu.cn (Q. Teng), kaiwang@glut.edu.cn (K. Wang), liangfupei@glut.edu.cn (F. Liang).
[1] These authors contributed equally to this work.

https://doi.org/10.1016/j.cclet.2022.108044
1001-8417/

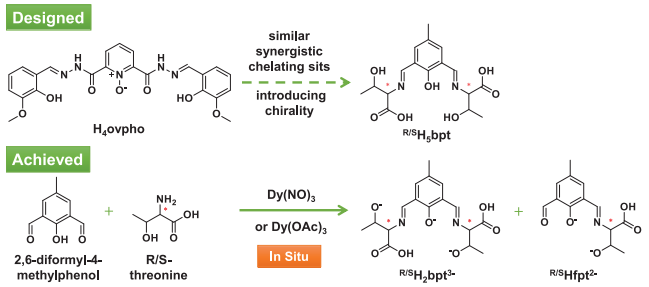

Scheme 1. The designed and achieved ligands in this work.

is reflected in the $O_{N\text{-}Oxide}$, which situates at centered parent and forms closely situated chelating pockets with two Schiff base arms synergistically. Its reactions with high equivalent lanthanide salts gave a series of novel high-nuclearity 4f clusters successfully [21,22]. Inspired by these works, we believed that the ligand featuring such special chelating structure would also be competent to assemble chiral high-nuclearity 4f clusters if it is endowed with the chirality. A novel Schiff base ligand of H_5btp was thus designed (Scheme 1, top). It is composed of a phenol parent and two homochiral threonine Schiff base arms, displaying a similar chelating structure as that of H_4ovpho ligand. In light of the effectiveness of free threonine in controlling the hydrolysis of 4f ions, which would favor the formation of high nuclearity lanthanide-oxo products [15,23,24], the designed H_5btp ligand was introduced through *in situ* synthetic approach starting from threonine and 2,6-diformyl-4-methylphenol.

As expected, two pairs of pure enantiomers of high-nuclearity 4f clusters with novel topologies, four-blade propeller shaped $\{Dy_{18}\}$ (**1R** and **1S**) and sandglass-like $\{Dy_9\}$ (**2R** and **2S**), were achieved successfully. They are all homochiral Dy-oxo clusters based on two kinds of *in situ* formed threonine Schiff base ligands. Strikingly, **1R** and **1S** are the second largest species in the chiral 4f cluster family with their nuclearity being next only to the reported $\{Er_{60}\}$ [15].

All clusters were synthesized from the reactions of Dy^{III} salts, 2,6-diformyl-4-methylphenol and threonine in a molar ratio of 8:1:2 in the presence of Et_3N. Their single crystals were obtained through the slow evaporation of organic-aqueous mixed solvents at room temperature (ESI). It revealed from all synthetic exploration that the *in situ* reaction condition is crucial for successful cultivation of single crystal samples. Rich oxo-bridges were generated in all clusters. It means that the hydrolysis of the Dy^{III} ions was controlled successfully in reaction process. The designed H_5btp ligand was formed *in situ* in all clusters as we expected. Unexpectedly, the H_3ftp ligand featuring single Schiff base arm was also formed in all clusters (Scheme 1, bottom), although the feeding molar ratio of 2,6-diformyl-4-methylphenol and threonine was controlled at 1:2 strictly. IR spectra analysis further confirmed the formation of these Schiff base ligands [25,26]. Charge balance calculation suggested that two kinds of ligands were deprotonated incompletely with the coordination forms of H_2btp^{3-} and $Hftp^{2-}$, respectively.

Clusters **1R** and **1S** are enantiomer with each other, so as **2R** and **2S**. Thus, only the structures of **1R** and **2R** are descripted in detail here. Cluster **1R** crystallizes in orthorhombic chiral space group of *I*222. It is made up of eighteen Dy^{III} ions, four $^{D}Hftp^{2-}$ and four $^{D}H_2btp^{3-}$ ligands, eight μ-OH^- ions, twenty μ_3-OH^- ions, a μ_6-O^{2-} ion, four NO_3^- ions, eight H_2O molecules, and several free solvent molecules. In the center of its molecule, six Dy^{III} ions are linked together by a μ_6-O^{2-} and eight μ_3-OH^- ions, forming an octahedral $[Dy_6(\mu_3\text{-}OH)_8(\mu_6\text{-}O)]^{8+}$ unit (Fig. 1a). Four triangular $[Dy_3(\mu_3\text{-}OH)]^{8+}$ units are located around this octahedral unit. Each of them is connected to the Dy4 ion locating at the equatorial plane of the octahedron unit through the bridging of two μ-OH^- and two μ_3-OH^- ions. An unprecedent four-blade propeller shaped $[Dy_{18}(\mu\text{-}OH)_8(\mu_3\text{-}OH)_{20}(\mu_6\text{-}O)]^{24+}$ core with a D_2-symmetry was thus assembled.

There are one $^{D}Hftp^{2-}$ and one $^{D}H_2btp^{3-}$ in each triangular $[Dy_3(\mu_3\text{-}OH)]^{8+}$ unit. The former bridges Dy1 and Dy2 with its O_{phenol}, displaying a μ-η^2:η^4 coordination mode (Fig. 1b). The latter shows a mode of μ_3-η^1:η^4:η^4 (Fig. 1c). It links the Dy1 and Dy3 within the same $[[Dy_3(\mu_3\text{-}OH)]^{8+}$ unit, and another Dy3 from the adjacent triangular $[Dy_3(\mu_3\text{-}OH)]^{8+}$ unit (Fig. 1c). The $[Dy_{18}(\mu_2\text{-}OH)_8(\mu_3\text{-}OH)_{20}(\mu_6\text{-}O)]^{24+}$ core is thus protected by the surrounding of four $^{D}Hftp^{2-}$ and four $^{D}H_2btp^{3-}$ ligands (Fig. 1d). The charge of whole cluster is further balanced by four NO_3^- ions, each of which coordinates to a Dy2 ion with a monodentate mode (Fig. 1e). In addition, there are twelve H_2O molecules coordinating to Dy2 and Dy5 ions, respectively, which further complete the ligation of whole cluster (Fig. 1e). Continuous symmetry measure (CShM) method was employed to evaluate exact coordination geometries of the Dy^{III} ion using SHAPE 2.1 software [27,28]. According to the CShM calculation (Tables S3-S5 in Supporting information), the Dy^{III} ions in **1R** exhibit three coordination geometries (Fig. S4 in Supporting information), namely nine-coordinated spherical capped square antiprism for Dy1 and Dy2, eight-coordinated triangular dodecahedron for Dy3, and nine-coordinated capped square antiprism for Dy4 and Dy5.

Although a considerable number of high-nuclearity 4f clusters have sprung up in recently years, such as $\{Gd_{48}\}$, $\{Er_{48}\}$, $\{Gd_{60}\}$, $\{Dy_{72}\}$, $\{Dy_{76}\}$, $\{Ln_{104}\}$, $\{Ln_{140}\}$ [29–35], reported chiral high-nuclearity 4f clusters were still sparse. A literature survey indicated that the existing chiral lanthanide clusters whose nuclearity are over 10 are only $\{La_{12}\}$, $\{Ln_{14}\}$ and $\{Er_{60}\}$ (Table S2) [14–18], with the $\{Er_{60}\}$ being the biggest one up to now. It follows that **1R** and **1S** could be the second largest members in chiral 4f cluster family so far.

Cluster **2R** crystallizes in monoclinic $P2_1$ space group. It consists of nine Dy^{III} ions, two $^{D}Hftp^{2-}$ and two $^{D}H_2btp^{3-}$ ligands, six OAc^- ions, ten μ_3-OH^- ions, six H_2O molecules, as well as an OAc^- counterion and several free solvent molecules. As shown in Fig. 2a, its sandglass-like $[Dy_9(\mu_3\text{-}OH)_{10}(OAc)_2]^{15+}$ skeleton contains two $\{Dy_5\}$ square pyramid units sharing a vertex ion (Dy5). Each triangular face of square pyramid unit is capped by a μ_3-OH^-group, by which eight Dy^{III} ions are linked to the Dy5 vertex. For four Dy^{III} ions on the base of each pyramid unit, three of them (Dy1, Dy2 and Dy3 or Dy6, Dy7 and Dy8) are linked together by a μ_3-OH^- ion, and the remaining one (Dy4 or Dy9) is bridged to one of its neighboring Dy^{III} ions (Dy1 or Dy6) by a μ-η^1:η^2 OAc^- ion. This constitutes the most remarkable feature that distinguish **2R** from other sandglass-like $\{Dy_9\}$ clusters [36–40]. In the previous reported sandglass-like $\{Dy_9\}$ clusters, four Dy^{III} ions on pyramid base were usually linked together by μ_4-OH^- and μ_5-O^{2-} ion (Table S5). Such unique bridging fashion in **2R** also resulted in considerable discrepancy for the distances between the adjacent Dy^{III} ions of pyramid base (Fig. 2a). However, the four Dy^{III} ions belonging to each pyramid base are still coplanar, with the RMSD value of 0.002 and 0.068, respectively.

The base of each square pyramid unit is further sheathed by a $^{D}Hftp^{2-}$ and a $^{D}H_2btp^{3-}$ ligands (Fig. 2d). The $^{D}Hftp^{2-}$ ligand adopts a μ-η^2:η^4 mode to link Dy1 with Dy2 (or Dy6 with Dy7) using its O_{phenol} (Fig. 2b). While the $^{D}H_2btp^{3-}$ ligand affords its O_{phenol} and one of $O_{carboxylate}$ to bridge Dy2, Dy3 and Dy4 (or Dy7, Dy8 and Dy9), displaying a μ_3-η^1:η^4:η^4 mode (Fig. 2c). Furthermore, there are six H_2O molecules and four OAc^- ions acting as the terminal ligands (Fig. 2e). They are one H_2O and one monodentate-coordinated OAc^- ion on Dy3, two H_2O and one bidentate-chelated

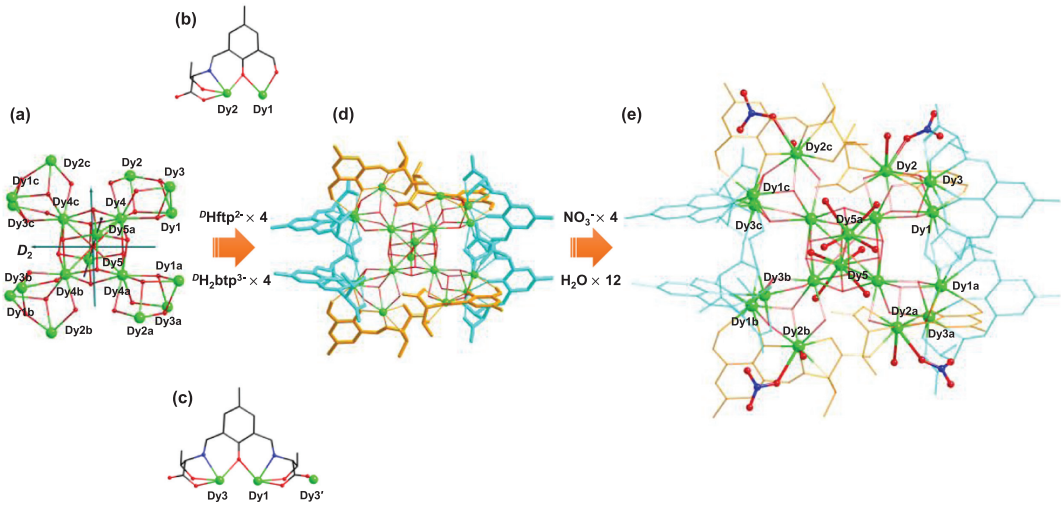

Fig. 1. (a) $[Dy_{18}(\mu\text{-OH})_8(\mu_3\text{-OH})_{20}(\mu_6\text{-O})]^{24+}$ core. (b) Coordination mode of $^{D}Hftp^{2-}$. (c) Coordination mode of $^{D}H_2btp^{3-}$. (d) Ligation of the ligands. (e) Whole cluster structure of **1R**. Symmetric codes: a, 1-*x*, 1-*y*, *z*; b, *x*, 1-*y*, 1-*z*; c, 1-*x*, *y*, 1-*z*.

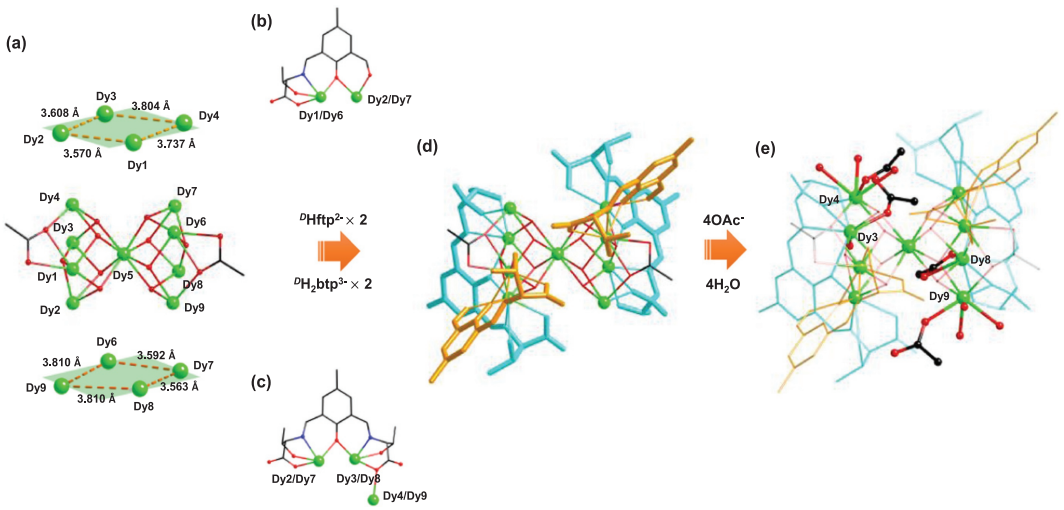

Fig. 2. (a) $[Dy_9(\mu_3\text{-OH})_{10}(OAc)_2]^{15+}$ skeleton. (b) Coordination mode of $^{D}Hftp^{2-}$. (c) Coordination mode of $^{D}H_2btp^{3-}$. (d) Ligation of the ligands. (e) $[Dy_9(^{D}Hftp)_2(^{D}H_2btp)_2(OAc)_6(\mu_3\text{-OH})_{10}(H_2O)_6]^{+}$ core of **2R**.

OAc^- ion on Dy4, one bidentate-chelated OAc^- ion on Dy8, and three H_2O and one monodentate-coordinated OAc^- ion on Dy9, respectively. All these ligands construct the cation core of $[Dy_9(^{D}Hftp)_2(^{D}H_2btp)_2(OAc)_6(\mu_3\text{-OH})_{10}(H_2O)_6]^{+}$ of **2R** on the basis of $[Dy_9(\mu_3\text{-OH})_{10}(OAc)_2]^{15+}$ skeleton. As suggested by calculated CShM values (Tables S6-S8 in Supporting information), the Dy^{III} ions in **2R** present three types of coordination geometries (Fig. S5 in Supporting information). The Dy1, Dy3 and Dy6 ions have spherical capped square antiprism geometries, while Dy2, Dy7 and Dy8 ions adopt spherical tricapped trigonal prism one, all of which are nine-coordinated. The Dy4, Dy5 and Dy9 ions were eight-coordinated, exhibiting square antiprism configurations.

Clusters **1R** and **1S** or **2R** and **2S** show strict mirror symmetry judged whether from the Dy-oxo skeletons and the binding modes of ligands, or from the whole molecular structures (Figs. S6 and S7 in Supporting information). Solid-state circular dichroism (CD) tests on their single crystal sample further support these results. As shown in Fig. 3, the CD spectra show obvious mirror symmetry effect whether **1R** *versus* **1S** or **2R** *versus* **2S**. Taking **2R** and **2S** as the examples, cluster **2R** exhibits two peaks with negative Cotton effect near 270 and 412 nm, and two peaks with positive Cotton effect near 318 and 366 nm. Correspondingly, four peaks can be observed in CD spectra of **2S**, which appear as the opposite Cotton effect in relative to those of **2R**. All these results are indicative of the homochirality of each cluster, and confirm that **1R** *versus* **1S** and **2R** *versus* **2S** are pairs of enantiomers, respectively.

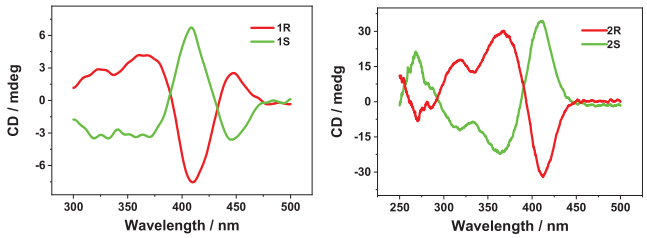

Fig. 3. Solid state CD spectra of all clusters.

The temperature dependence of magnetic susceptibilities was measured in the range of 300–2 K with an applied dc field of 1 kOe (Fig. S8 in Supporting information). At room temperature, the $\chi_M T$ values of **1R**, **1S**, **2R** and **2S** are 254.81, 254.12, 128.25 and 128.09 cm^3 K/mol, respectively, being close to their corresponding theoretical values for eighteen or nine isolated Dy^{III} ions

($J = 5/2$, $g = 4/3$). Upon cooling, the $\chi_M T$-T curves all show gradually decreasing tendency, finally reaching the minimums of 153.36, 164.54, 73.74 and 74.66 cm^3 K/mol at 2 K, respectively. This could be ascribed to the contributions of thermal depopulation effect of Stark sublevels of Dy^{III} ions and also possible antiferromagnetic couplings between the Dy^{III} ions within cluster [41]. Furthermore, the $\chi_M T$-T curve of each cluster was almost coincided with that of its enantiomer. It's no surprise that the chiral isomerization did not induce substantial change of magnetic structures. At different temperatures, the field dependence of the magnetization (M) of all clusters were collected in the field (H) range of 0–70 kOe (Fig. S9 in Supporting information). The M-H curves of all clusters revealed a slow rise of M along with the increasing of H. The maximum of M values appeared at 70 kOe and 2 K, but didn't reach saturation. And the M-H curves recorded at different temperature are not overlapped. These behaviors suggest the presence of low-lying excited states and/or magnetic anisotropy of the Dy^{III} ions in all clusters [42].

In conclusion, we have succeeded in the synthesis of two pairs of chiral high nuclearity 4f clusters based on threonine Schiff base ligands. The hydrolysis of Dy^{III} ions were successfully controlled in introducing the chiral source through *in situ* synthesis method. This contributes to the formation of rich oxo-bridges, which construct unprecedent four-blade propeller shaped $\{Dy_{18}\}$ and new sandglass-like $\{Dy_9\}$ Dy-oxo skeletons together with chiral threonine Schiff bases ligands. Magnetic investigation revealed possible antiferromagnetic interactions between the Dy^{III} centers of each cluster. This work thus affords novel and rare members of chiral high nucleartiy 4f clusters, as well as an efficient synthesis strategy towards these clusters.

Declaration of competing interest

The authors declare that they have no known competing financial interests or personal relationships that could have appeared to influence the work reported in this paper.

Acknowledgments

This work was financially supported by the National Natural Science Foundation of China (Nos. 21961008, 22271068, 22075058 and 22261012), Guangxi Science and Technology Base and Talents Program (No. AD21220105), and Guangxi Natural Science Foundation (No. 2022GXNSFBA035472).

Supplementary materials

Supplementary material associated with this article can be found, in the online version, at doi:10.1016/j.cclet.2022.108044.

References

[1] W. Huang, X. Ma, O. Sato, et al., Chem. Soc. Rev. 50 (2021) 6832–6870.
[2] Y. Jin, C. Zhang, X.Y. Dong, S.Q. Zang, T.C.W. Mak, Chem. Soc. Rev. 50 (2021) 2297–2319.
[3] Y. Zou, Q. Gao, N. Sun, et al., Chin. Chem. Lett. 34 (2023) 107390.
[4] C.M. Liu, R.G. Xiong, D.Q. Zhang, D.B. Zhu, J. Am. Chem. Soc. 132 (2010) 4044–4045.
[5] Z.L. Chen, Y.L. Shen, L.L. Li, et al., Dalton Trans. 46 (2017) 15032–15039.
[6] Q.P. Li, J.J. Qian, C.B. Tian, et al., Dalton Trans. 43 (2014) 3238–3243.
[7] Y.J. Zhang, G. Wu, H. Xu, et al., Inorg. Chem. 59 (2020) 193–197.
[8] M.M. Zhang, X.Y. Dong, Z.Y. Wang, et al., J. Am. Chem. Soc. 143 (2021) 6048–6053.
[9] G. Bozoklu, C. Gateau, D. Imbert, et al., J. Am. Chem. Soc. 134 (2012) 8372–8375.
[10] L. Riccardi, F.D. Biasi, M.D. Vivo, et al., ACS Nano 13 (2019) 7127–7134.
[11] X.L. Tang, W.H. Wang, W. Dou, et al., Angew. Chem. Int. Ed. 48 (2009) 3499–3502.
[12] Y.B. Tan, Y. Okayasu, S. Katao, et al., J. Am. Chem. Soc. 142 (2020) 17653–17661.
[13] C.F. Zhu, H.T. Tang, K.K. Yang, et al., J. Am. Chem. Soc. 143 (2021) 12560–12566.
[14] C. Zhao, Q.F. Sun, W.M. Hart-Cooper, et al., J. Am. Chem. Soc. 135 (2013) 18802–18805.
[15] X.J. Kong, Y.L. Wu, L.S. Long, L.S. Zheng, Z.P. Zheng, J. Am. Chem. Soc. 131 (2009) 6918–6919.
[16] X.L. Li, L.F. He, X.L. Feng, et al., CrystEngComm 11 (2011) 3643–3645.
[17] T.Q. Lu, J.J. Yin, C. Chen, et al., CrystEngComm 39 (2021) 6923–6929.
[18] H.L. Zhao, D.X. Cui, J.N. Kou, et al., Chin. J. Chem. 40 (2022) 1165–1170.
[19] N.M. Parekh, B.M. Mistry, M. Pandurangan, et al., Chin. Chem. Lett. 28 (2017) 602–606.
[20] G.T. Vidyavathi, B.V. Kumar, A.V. Raghu, et al., J. Mol. Struct. 1249 (2022) 131656.
[21] K. Wang, Z.L. Chen, H.H. Zou, et al., Chem. Commun. 52 (2016) 8297–8300.
[22] K. Wang, Z.L. Chen, H.H. Zou, et al., Dalton Trans. 47 (2018) 2337–2343.
[23] Z.P. Zheng, Chem. Commun. 24 (2001) 2521–2529.
[24] D.T. Thielemann, I. Fernández, P.W. Roesky, Dalton Trans. 29 (2010) 6661–6666.
[25] A.V. Raghu, G.S. Gadaginamath, T.M. Aminabhavi, J. Appl. Polym. Sci. 98 (2005) 2236–2244.
[26] A.V. Raghu, G.S. Gadaginamath, H.M. Jeong, J. Appl. Polym. Sci. 113 (2009) 2747–2754.
[27] H. Zabrodsky, S. Peleg, D. Avnir, J. Am. Chem. Soc. 114 (1992) 7843–7851.
[28] M. Pinsky, D. Avnir, Inorg. Chem. 37 (1998) 5575–5582.
[29] F.S. Guo, Y.C. Chen, L.L. Mao, et al., Chem. Eur. J. 19 (2013) 14876–14885.
[30] W.M. Huang, W.M. Chen, Q.X. Bai, et al., Angew. Chem. Int. Ed. 61 (2022) e202205385.
[31] X.M. Luo, Z.B. Hu, Q.F. Lin, et al., J. Am. Chem. Soc. 140 (2018) 11219–11222.
[32] L. Qin, Y.Z. Yu, P.Q. Liao, et al., Adv. Mater. 28 (2016) 10772–10779.
[33] X.Y. Li, H.F. Su, Q.W. Li, et al., Angew. Chem. Int. Ed. 58 (2019) 10184–10188.
[34] J.B. Peng, X.J. Kong, Q.C. Zhang, et al., J. Am. Chem. Soc. 136 (2014) 17938–17941.
[35] X.Y. Zheng, Y.H. Jiang, G.L. Zhuang, et al., J. Am. Chem. Soc. 139 (2017) 18178–18181.
[36] P. Hu, L.H. Cao, A.G. Liu, et al., Dalton Trans. 50 (2021) 12814–12820.
[37] D.I. Alexandropoulos, S. Mukherjee, C. Papatriantafyllopoulou, et al., Inorg. Chem. 50 (2011) 11276–11278.
[38] X.B. Xu, L. Zhao, G.F. Xu, et al., Dalton Trans. 24 (2011) 6440–6444.
[39] H.H. Zou, L.B. Sheng, Z.L. Chen, F.P. Liang, Polyhedron 88 (2015) 110–115.
[40] M.A. Singh-Wilmot, R.A. Sinclair, M. Andrews, et al., Polyhedron 53 (2013) 187–192.
[41] W.P. Chen, G.J. Zhou, Z.L. Gou, et al., Chin. Chem. Lett. 32 (2021) 838–841.
[42] S.R. Li, Z.Z. Weng, L.P. Jiang, et al., Chin. Chem. Lett. 34 (2023) 107251.